

# Fibroblast Growth Factor-23 Mutants Causing Familial Tumoral Calcinosis Are Differentially Processed

Tobias Larsson, Siobhan I. Davis, Holly J. Garringer, Sean D. Mooney, Mohamad S. Draman, Michael J. Cullen, and Kenneth E. White

Department of Medical and Molecular Genetics (T.L., S.I.D., H.J.G., S.D.M., K.E.W.), Indiana University School of Medicine, Indianapolis, Indiana 46202; and Department of Endocrinology (M.S.D., M.J.C.), Saint James's Hospital and Trinity College Dublin Medical School, Dublin 8, Ireland

Familial tumoral calcinosis (TC, OMIM 211900) is a heritable disorder characterized by hyperphosphatemia, normal or elevated serum 1,25-dihydroxyvitamin D, and often severe ectopic calcifications. Two recessive mutations in *fibroblast growth factor-23* (*FGF23*), serine 71/glycine (S71G) and serine 129/phenylalanine (S129F), were identified as causing TC. Herein, we undertook comprehensive biochemical analyses of an extended TC family carrying the S71G *FGF23* mutation, which revealed that heterozygous (serine/glycine, S/G) individuals had elevated serum *FGF23* C-terminal fragments compared with wild-type (serine/serine, S/S) family members ( $P < 0.025$ ). To understand the differential processing of *FGF23* in TC patients, we transiently expressed S71G as well as S129F *FGF23*. *FGF23* ELISA in tandem with Western analyses revealed increased proteolytic cleavage of mutant *FGF23* and a

limited secretion of intact protein. Furthermore, S71G and S129F *FGF23* carrying mutations that disrupt the furin-like protease RXXR motif in *FGF23* rescued the secretion of the intact protein, and both TC mutant proteins harboring the R176Q mutation revealed no altered sensitivity to trypsin compared with the native (R176Q)*FGF23*. Finally, S71G, but not S129F mutant *FGF23*, is rescued by temperature. In summary, *FGF23* mutations causing TC lead to increased intracellular proteolysis of *FGF23*, most likely by furin-like proteases, due to conformational changes of the mutant protein. The destabilizing nature of these mutations provides new insight into the pathophysiology of TC and exemplifies the physiological importance of *FGF23* in phosphate and vitamin D metabolism. (*Endocrinology* 146: 3883–3891, 2005)

**F**IBROBLAST GROWTH FACTOR-23 (*FGF23*) is a circulating factor that plays a critical role in phosphate (Pi) and vitamin D metabolism, as evidenced by the fact that *FGF23* missense mutations cause autosomal dominant hypophosphatemic rickets (ADHR) (1). ADHR is characterized by hypophosphatemia with inappropriately normal 1,25-dihydroxyvitamin D ( $1,25\text{-(OH)}_2\text{D}_3$ ) concentrations, as well as bone pain, fracture, and rickets (2, 3). This phenotype parallels that seen in patients with tumor-induced osteomalacia and X-linked hypophosphatemic rickets, in whom elevated serum *FGF23* levels are often observed (4–6). Delivery of either recombinant wild-type or ADHR mutant *FGF23* to rodents (7–9) or overexpressing *FGF23* in transgenic mice (10–12) results in hypophosphatemia secondary to renal Pi wasting, indicating that *FGF23* is a phosphaturic factor. Conversely, *Fgf23* null mice are hyperphosphatemic with increased renal Pi reabsorption due to increased expression of the type II renal  $\text{Na}^+$ /Pi cotransporter (Npt2a) (13, 14).

Investigation into the role of *FGF23* in vitamin D homeostasis has determined that *FGF23* is a potent regulator of key enzymes involved in vitamin D metabolism. Delivery of excess *FGF23* *in vivo* suppresses renal vitamin D  $1\text{-}\alpha$  hydrox-

ylase (OHase) mRNA levels (7–9) and increases the vitamin D  $25\text{-OHase}$  mRNA (8, 9). These actions on vitamin D metabolism most likely contribute to the suppressed serum  $1,25\text{-(OH)}_2\text{D}_3$  levels in ADHR, tumor-induced osteomalacia, and X-linked hypophosphatemic rickets patients. Homozygous *Fgf23* null mice demonstrate marked elevation of serum  $1,25\text{-(OH)}_2\text{D}_3$  levels due to increased renal expression of  $1\alpha\text{-OHase}$  mRNA (13, 14) further supporting an essential role for *FGF23* in vitamin D metabolism.

Familial tumoral calcinosis (TC) is a heritable metabolic disorder characterized by ectopic calcified tumoral masses and dental abnormalities, as well as soft tissue periarticular and vascular calcifications (15, 16). Biochemical abnormalities include hyperphosphatemia, increased tubular reabsorption of Pi, and normal or elevated  $1,25\text{-(OH)}_2\text{D}_3$  concentrations. Despite these abnormalities, calcium and PTH are usually within the normal reference ranges (17). The TC phenotype is similar to that described in *Fgf23* knockout mice (13, 14). Importantly, we (18) and others (19) recently demonstrated that a recessive homozygous mutation in the *FGF23* gene, giving rise to an amino acid change from a serine to a glycine at residue 71 (S71G), causes familial TC. Furthermore, in a preliminary report, another *FGF23* mutation was identified as giving rise to an amino acid change from a serine to a phenylalanine at residue 129 (S129F), which leads to hyperphosphatemia, high serum  $1,25\text{-(OH)}_2\text{D}_3$ , and a calcification phenotype characteristic of TC (20). Therefore, it is likely that the S71G and S129F mutations compromise normal function of the wild-type *FGF23* protein, which is

First Published Online June 16, 2005

Abbreviations: ADHR, Autosomal dominant hypophosphatemic rickets;  $1,25\text{-(OH)}_2\text{D}_3$ , 1,25-dihydroxyvitamin D; *FGF23*, fibroblast growth factor-23; OHase, hydroxylase; Pi, phosphate; SIFT, sorting intolerant from tolerant; TC, tumoral calcinosis.

*Endocrinology* is published monthly by The Endocrine Society (<http://www.endo-society.org>), the foremost professional society serving the endocrine community.

consistent with the serum biochemistry and calcification profiles of TC patients as well as the *Fgf23* knockout mice (18, 19).

At present, it is unclear whether the S71G *FGF23* mutations lead to TC by haploinsufficiency or if individuals heterozygous (serine 71/glycine 71, S/G) for the S71G mutation are unaffected. Therefore, in the current study, we aimed to identify the genotype-phenotype correlations of an expanded TC kindred and to explore the functional consequences of the known TC *FGF23* mutations. Herein, we examined the largest TC family with *FGF23* mutations to date and demonstrate that the S71G and S129F substitutions confer increased intracellular proteolytic degradation of FGF23, likely due to conformational changes of the mutant protein.

## Materials and Methods

### TC patients

All patients provided written, informed consent in accord with the Institutional Review Board of Indiana University. This family is of Caucasian origin and has, in part, previously been described (18, 21).

### Serum biochemistries

Routine serum biochemistries were assessed by standard protocols. 1,25-(OH)<sub>2</sub>D<sub>3</sub> concentrations were measured using the 1,25-(OH)<sub>2</sub>D<sub>3</sub> RIA kit (DiaSorin, Stillwater, MN). Serum intact FGF23 concentrations were assessed using an ELISA according to the manufacturer's protocol (Kainos Laboratories International, Tokyo, Japan). This two-site, monoclonal antibody ELISA has previously been shown to recognize human and rodent FGF23/*Fgf23* (4). Serum FGF23 concentrations were also evaluated using the Immotopics, Inc. (San Clemente, CA) C-terminal FGF23 serum assay kit according to the manufacturer's instructions. This kit is a two-site sandwich ELISA-based assay that recognizes the C-terminal portion of FGF23 (5).

### FGF23 mutational analysis

Genomic DNA was extracted from blood samples using the Qiamp DNA Blood Extraction kit (Qiagen, Inc., Valencia, CA) according to the manufacturer's protocol. The three *FGF23* exons, including the intron-exon splice junctions, were PCR-amplified with intronic primers: (Exon 1, forward: 5'-aatctcagcaccagccactc-3', reverse: 5'-gatggacaacaagggtgctc-3'; Exon 2, forward: 5'-ttcaggaggtgcttgaagg-3', reverse: 5'-ttgcaaatggtgaccaacac-3'; and Exon 3, forward: 5'-cttcacgtggttcgctcttg-3', reverse: 5'-tgctgagggtggttaag-3') using 20 ng of genomic DNA as templates. PCR conditions for all experiments were: 1 min at 95 C; followed by 35 cycles of 1 min at 95 C, 1 min at 57 C, 1 min at 72 C; and a final extension of 7 min at 72 C. Amplified exons were analyzed by DNA sequencing with the appropriate forward primers for each *FGF23* exon using Big Dye Terminator Chemistry or the [<sup>33</sup>P]ddNTP ThermoSequenase kit (USB, Inc., Cleveland, OH).

### Expression vectors

The cDNA encoding human FGF23 was amplified from normal human tissue RNA as previously described (22) and cloned into the pcDNA3.1(+) vector (Invitrogen, Carlsbad, CA). To create N-terminal FLAG (residues DYKDDDDK)-tagged FGF23 fusion constructs containing FGF23 amino acids 25–251, the pcDNA3.1(+)(FGF23) vector was amplified with the primers: forward (contains *Eco*RI site, underlined) 5'-ggaattcatatccaatgctctccca-3' and reverse (contains *Bam*HI site, underlined) 5'-cgggatccctagatgaacttggcga-3'. The resulting cDNAs were digested with *Eco*RI and *Bam*HI, and directionally ligated into the pFLAG-CMV-3 expression vector (Sigma-Aldrich, Inc., St. Louis, MO), which allows secretion of N-terminal FLAG-tagged fusion proteins. The following mutant FLAG-tagged FGF23 constructs, with either the TC mutations alone, or in combination with the known ADHR mutations R176Q and R179Q, were prepared using the QuickChange II XL Site-Directed Mutagenesis Kit (Stratagene, Cedar Creek, TX): 1) (S71S)(R176Q)FGF23; 2a) (S71G)FGF23; 2b) (S71G)(R176Q)FGF23; 2c)

(S71G)(R176 + 179Q)FGF23; 3a) (S129F)FGF23; 3b) (S129F)(R176Q)FGF23; 3c) (S129F)(R176 + 179Q)FGF23. All constructs were sequenced to confirm the proper reading frame of the fusion protein and the correct introduction of mutations.

### Plasmid purification and DNA sequencing

Plasmids were isolated with the Qiagen Mini- and Maxi-Prep Kits (Qiagen, Inc.) according to the manufacturer's instructions and subjected to sequencing using the Big Dye Terminator Chemistry or the ThermoSequenase Kit (USB, Inc.) with [<sup>33</sup>P]ddNTP incorporation. Sequenced products were separated on a standard 0.2 mm, 6% polyacrylamide gel and autoradiography was performed.

### Cell culture

HEK293 cells (American Type Culture Collection, Manassas, VA) were cultured in DMEM (Life Technologies, Inc., Rockville, MD) with 10% fetal bovine serum (Hyclone, Logan, UT), 1 mM sodium pyruvate, 25 mM HEPES buffer, L-glutamine and penicillin-streptomycin at 37 C and 5% CO<sub>2</sub>. For temperature rescue experiments, cells were grown at 29 C and 5% CO<sub>2</sub>.

### Transient transfections

HEK293 cells (1.2 × 10<sup>6</sup>) were seeded on 60-mm culture dishes (Fisher, Inc., Pittsburgh, PA) and transiently transfected in serum-free media with the Eugene 6 reagent (Hoffmann-La Roche, Inc., Nutley, NJ) using 2 μg of plasmid DNA according to the manufacturer's instructions. Transfection efficiency was assessed by cotransfection of a β-galactosidase reporter plasmid and X-gal staining by standard protocols. After transfection, the incubation was continued for an additional 48 h. For some samples, conditioned media were concentrated 5–60× with Macrosepomega 10-K concentrators (VWR, Batavia, IL) at 4 C, as indicated in the figures.

### Endoproteolytic digestions

Conditioned media containing the (S71S)(R176Q)FGF23 or (S71G)(R176Q)FGF23 and (S129F)(R176Q)FGF23 were subjected to trypsin digestion (0, 4, 8, 16, and 32 ng/μl) for 1 h at room temperature. Final reaction volumes were 50 μl, and the volume of FGF23-conditioned media was adjusted to equalize total protein content between the samples. The digests were analyzed by Western blotting as described below.

### Western analysis

Protein samples and standards for molecular mass determination were electrophoresed on 15% SDS-PAGE mini-gels (Bio-Rad Inc., Hercules, CA) and electrotransferred onto PVDF membranes (Bio-Rad Inc.). Membranes were incubated with 2.5 μg/ml antihuman FGF23 polyclonal antibody (kindly provided by Immotopics, Inc.). The polyclonal antibody is an affinity-purified IgG to FGF23 residues 225–244 that recognizes recombinant human FGF23 protein by Western analysis. For detection of N-terminal fragments, membranes were incubated with 2.5 μg/ml of an anti-FLAG M2 monoclonal antibody (Sigma-Aldrich, Inc.). Blots were incubated with donkey antigoat-HRP (1:5000) (Santa Cruz, Inc., Santa Cruz, CA) or goat antimouse-HRP (1:3000) antibodies (Bio-Rad Inc.) and visualized by enhanced chemiluminescence (Amersham Inc., Piscataway, NJ).

### Molecular modeling

The x-ray crystallographic structures for the homologous proteins, FGF19 (23) and FGF1, have been previously determined. These structures were visualized using UCSF Chimera ([www.cgl.ucsf.edu/chimera](http://www.cgl.ucsf.edu/chimera)), and the mutation positions in FGF23 were mapped based on the multiple alignment published previously (1). A predicted structural model of FGF23 was also determined from MODBASE (24) and the structural environment of the serine 71 and serine 129 positions were assessed accordingly. SIFT (sorting intolerant from tolerant) analysis was performed as described (<http://blocks.fhcr.org/sift/SIFT.html>).

### Statistical analysis

Differences in biochemical parameters between S/S and S/G family members were calculated using Student's independent *t* test. All values are expressed as mean  $\pm$  SEM. A *P* value less than 0.05 was considered to be statistically significant.

## Results

### Genotype/phenotype correlations of the S71G FGF23 TC family

We have previously presented a portion of this TC family pedigree and the phenotypes for the affected individuals in generation V (18). These affected individuals were confirmed negative for mutations in the *GALNT3* gene and positive for a homozygous S71G mutation in *FGF23* (glycine 71/glycine 71, G/G) (18). In the present study, we expanded this pedigree and determined the genotype-phenotype correlations for the entire kindred. These studies revealed that two family members in generation V and three members in generation VI were heterozygous carriers of the S71G mutation (Fig. 1). Notably, these individuals appeared grossly normal with no obvious phenotype involving disturbed Pi homeostasis or vitamin D metabolism (serum biochemistries for the TC kindred are summarized in Table 1). Furthermore, heterozygotes had no prior medical record of lower back pain or other symptoms and signs of ectopic calcifications. Importantly, the carriers also presented with normal intact serum FGF23 ( $14.0 \pm 1.9$  vs.  $15.7 \pm 2.3$  pg/ml) but slightly elevated C-terminal FGF23 ( $74.1 \pm 5.5$  vs.  $54.6 \pm 4.7$  reference units/ml,  $P < 0.025$ ) compared with family members expressing both wild-type *FGF23* alleles (Fig. 2). Moreover, there were no significant differences in serum Pi, calcium, PTH, or  $1,25\text{-(OH)}_2\text{D}_3$  levels between S/S and S/G family members. This

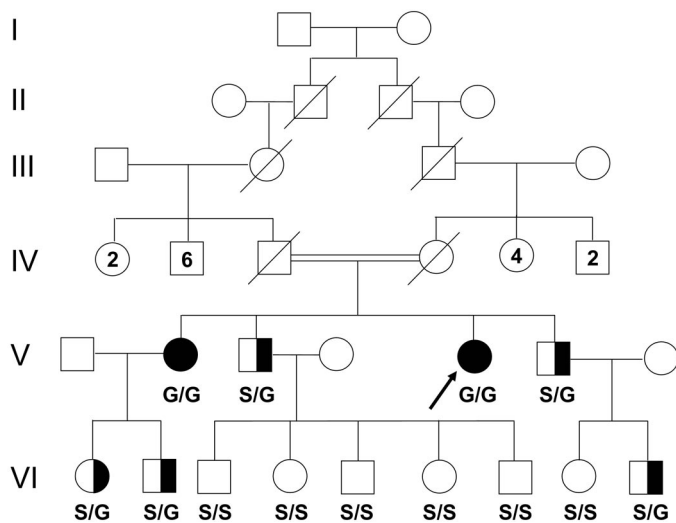


FIG. 1. Pedigree of the TC family. The genotype for each family member examined is displayed as follows: S/S (wild type); S/G (heterozygote); G/G (homozygote). Filled symbols denote a TC disease phenotype and half-filled symbols indicate heterozygous carriers of the S71G mutation. The generations of the family are denoted by Roman numerals and the arabic numerals within the symbols indicate number of children of a gender. The connecting lines between the two deceased parents in generation IV of the TC patients homozygous for the S71G FGF23 mutation indicate that the family is consanguineous. The proband of the TC family in generation V is marked by the black arrow.

observation is in stark contrast to the two G/G TC family members that presented with ectopic calcification in the vertebral discs, soft tissue of the thighs and large arteries leading to premature peripheral vascular ischemia (21). The vascular calcification observed in the brachial arteries as well as lower limb vessels is evenly distributed, which is an uncommon feature of vascular calcific deposits. Furthermore, these affected individuals displayed low-normal intact FGF23 but markedly elevated C-terminal FGF23 as previously reported (18) (Fig. 2). Taken together, these data suggest that there is no gene-dosage effect in TC arising from mutations in *FGF23*, and that although C-terminal FGF23 fragments were elevated in the carriers of the S71G mutation, one normal *FGF23* gene copy is sufficient to maintain normal regulation of Pi and vitamin D homeostasis.

### Expression of wild-type and mutant FGF23 cDNAs

To follow up our results that S71G mutant FGF23 results in increased C-terminal fragments in our TC kindred, we sought to explore the functional consequences of the S71G mutation as well as the previously reported S129F *FGF23* mutation (20). In this regard, we expressed the wild-type, S71G, and S129F mutant FGF23 proteins by transient transfection in HEK293 cells and analyzed conditioned media and cell lysates by Western blotting. Unconcentrated conditioned media from cells expressing FLAG-tagged wild-type FGF23 revealed two migrating bands of 36 and 15 kDa in agreement with previous reports (25, 26), whereas media from cells expressing S71G and S129F mutant FGF23 revealed no immunoreactivity when using the C-terminal antibody for detection (Fig. 3A). Despite a 60-fold concentration, we were unable to detect C-terminal fragments in the media from cells expressing the S71G and S129F mutant proteins using either our C-terminal antibody or a previously described polyclonal C-terminal antibody raised against residues 206–222 of human FGF23 (22) for detection (data not shown). Because the small C-terminal fragments could have been lost during electrotransfer, we then used a monoclonal mouse anti-FLAG antibody to determine whether N-terminal FGF23 fragments were detectable in the conditioned media. Unconcentrated conditioned media from cells transfected with wild-type or concentrated conditioned media containing mutant FGF23 revealed the intact 36-kDa band as well as a 26-kDa band representing the portion of FGF23 N-terminal of the furin-like protease R176XXR179 cleavage site, similar to our earlier results (22) (Fig. 3B). The immunoreactivity was much weaker in the two mutants, as they required a 30–60 $\times$  concentration to reveal the FGF23 bands, indicating lower secretion of intact FGF23.

To explore the possibility of improper processing of S71G and S129F mutant FGF23, we performed Western blotting on cell lysates from the corresponding transient transfections. A 32-kDa FGF23 species, slightly smaller than that observed in conditioned medium, was present in both cell lysates from S71G or S129F mutant FGF23, whereas only slight immunoreactivity was present in the lysates containing wild-type FGF23 protein (Fig. 3A). This indicated that both S71G and S129F mutant FGF23 proteins have a defect in secretion and/or in intracellular trafficking, consistent with an earlier



**TABLE 1.** Serum biochemistries of the TC family

FGF23 genotype	Phosphate 2.7–4.5 mg/dl (0.8–1.4 mmol/liter)	Calcium 8.82–10.42 mg/dl (2.20–2.60 mmol/liter)	PTH 10–65 pg/ml	1,25(OH) <sub>2</sub> D <sub>3</sub> (24–154 pmol/liter)
G/G (n = 2)	6.37 ± 0.27 (2.06 ± 0.09)	10.80 ± 0.020 (2.70 ± 0.0050)	11 ± 0.5	(97 ± 37)
S/G (n = 5) <sup>a</sup>	3.19 ± 0.36 (1.03 ± 0.12)	9.94 ± 0.20 (2.49 ± 0.049)	15 ± 1.7	(96 ± 15)
S/S (n = 6)	3.26 ± 0.25 (1.05 ± 0.08)	10.23 ± 0.16 (2.56 ± 0.039)	12 ± 1.6	(98 ± 12)

Values are expressed as mean ± SEM. SI units are displayed in *parentheses*. As described, the two G/G individuals revealed hyperphosphatemia and mild hypercalcemia.

<sup>a</sup> No significant differences in serum biochemistries were observed between S/G and S/S family members.

report of S71G mutant FGF23 being retained in the Golgi complex (19). The discrepancy in molecular weight between the full-length protein in cell lysates and in the media may represent additional glycosylation of the mature, secreted protein.

To determine the relative levels of intact *vs.* C-terminal FGF23 in the conditioned media from cells expressing the mutant FGF23s, we performed ELISA measurements of the media using a C-terminal assay that recognizes both the full-length and C-terminal portions of FGF23 (5) and an intact FGF23 serum assay (4). These results demonstrate that conditioned media from cells expressing wild-type or the S71G and S129F FGF23 mutants all contained FGF23 levels above the upper assay limit when measured with the C-terminal ELISA. However, both mutants produced very low amounts of intact FGF23 compared with wild-type protein (Fig. 4). As expected, when wild-type FGF23 is cotransfected with S71G FGF23, the levels of intact protein produced are above the assay upper limits (not shown). These observations parallel our findings in serum from our TC family (18) (Fig. 2), *i.e.* that S71G mutant FGF23 is differentially processed compared

with wild-type FGF23, resulting in increased levels of C-terminal fragments, and that heterozygote individuals are capable of producing intact wild-type FGF23 although they possess one S71G allele. Our failure to detect any C-terminal fragments in the unconcentrated conditioned media from cells expressing S71G and S129F mutant FGF23s by Western blotting (Fig. 3A) indicate that numerous C-terminal fragments, smaller than 15 kDa, are likely present in the media. These differences between the ELISA and Western analyses may be due to secretion of smaller fragments generated by intracellular processing of intact FGF23, or because the S71G

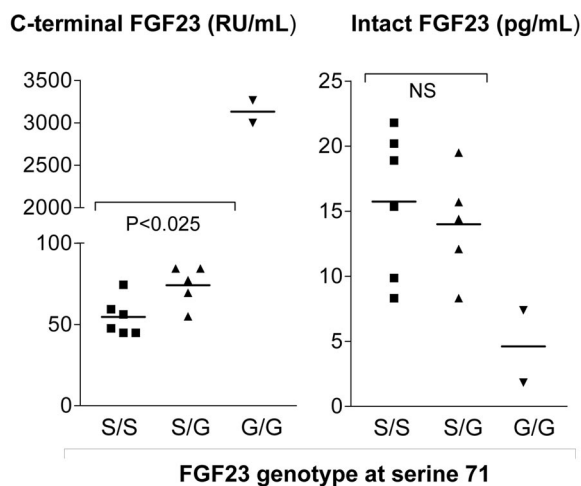


**FIG. 2.** Serum FGF23 levels in the TC family. FGF23 levels as determined by the C-terminal ELISA (*left*) were markedly elevated in the affected G/G individuals, whereas a small but significant elevation was noted in S/G family members compared with those with the S/S genotype. The G/G individuals displayed low-normal intact FGF23 levels (*right*) in contrast to S/G family members that revealed normal intact FGF23 levels compared with those with the S/S genotype.

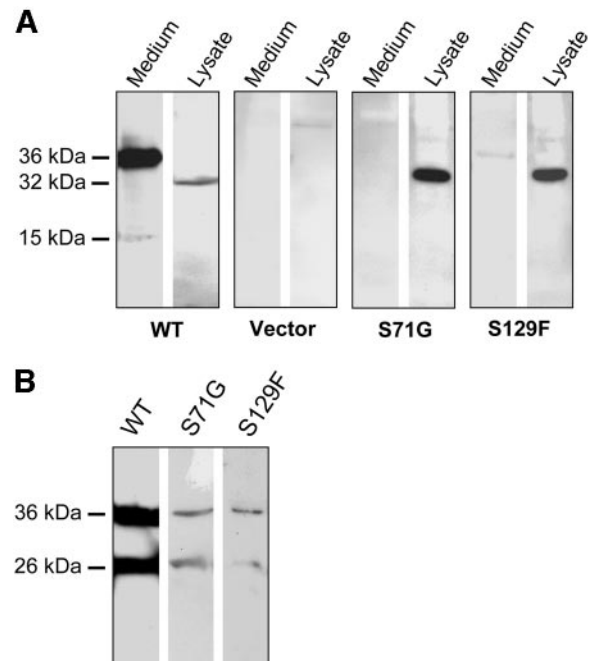


**FIG. 3.** Western blotting of wild-type and mutant FGF23. A, Wild-type FGF23 medium produced two bands of 36 and 15 kDa when assessed with the C-terminal anti-FGF23 antibody. Medium from cells expressing empty vector or mutant FGF23 revealed no immunoreactivity in contrast to the cell lysates of both mutant FGF23 that produced a distinct 32-kDa band. All media were unconcentrated in A. S71G and S129F media were concentrated 30 times in B. B, Conditioned media were analyzed using a monoclonal FLAG-antibody, which detects the N-terminal FLAG-tagged epitope of wild-type and mutant FGF23 protein. Two bands of 36 and 26 kDa were detected, corresponding to intact FGF23 and the portion N-terminal to the R176 cleavage site, respectively.

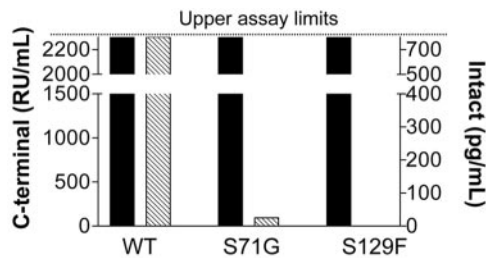


FIG. 4. FGF23 ELISA measurements of conditioned media. Conditioned media from cells expressing wild-type and mutant FGF23 were analyzed with both a C-terminal (left *y*-axis) and an intact (right *y*-axis) ELISA. Black bars represent C-terminal values and hashed bars represent intact values. Note that C-terminal FGF23 levels were above the assay range for both the wild-type and the FGF23 mutants, in contrast to low or undetectable intact FGF23 levels in the same mutant samples.

and S129F proteins are more rapidly degraded than wild-type FGF23 postsecretion.

#### Molecular modeling of wild-type and mutant FGF23

To assess the structural environment of position S71 and S129 in FGF23, an analysis of the known crystal structure of FGF19 was used, which is predicted to be similar to FGF23 (23). This structure of FGF19 (pdb:1PWA) was determined at 1.9 Å resolution (23). An initial analysis was performed using this structure for FGF19 and a comparative model of FGF23 from MODBASE (24). Based upon the FGF19 structure, S78 is analogous to S71 in FGF23, is predicted to be slightly buried, and lies within a short  $\alpha$  helical segment that is between two antiparallel  $\beta$  sheets. The sidechain of S78 potentially forms hydrogen bonds with a water molecule, S75, and H46. These residues are conserved in FGF23 as T68 and H41 and mutation of position 71 to a glycine would disrupt these molecular interactions with these residues and may lead to FGF23 destabilization. A similar analysis was performed on position S129. In FGF19, this position is conserved as S136, and the polar side chain potentially hydrogen bonds with a water molecule and loop amino acids K138 and H139 in the turn between  $\beta$  sheets 9 and 10. These amino acids are not completely conserved between FGF19 and FGF23, as the residues at these positions are Q131 and Y132, respectively. Mutation of position 129 to a phenylalanine may accordingly also lead to destabilization because of disruption of sidechain hydrogen bonding between S129 and these key residues. Of note, SIFT and secondary structure prediction software previously demonstrated that the S71G mutation produced a substitution intolerance score of 0.01 (a score less than 0.05 predicts decreased stability) (18). Extended SIFT analysis with FGF23 containing the S129F mutation revealed a substitution intolerance score of 0.00, indicating that the S129F mutation may mechanistically be even more unstable than the S71G mutation (data not shown).

#### Rescue of mutant protein by introducing R176Q or (R176 + 179Q) mutations

To determine the mechanism of the increased production of secreted FGF23 fragments as a result of the TC mutations,

we investigated whether an endogenous furin-like enzyme activity is involved in the degradation of S71G or S129F mutant FGF23. In this regard, we coexpressed either the R176Q or a (R176 + 179Q) double mutant in tandem with the S71G or the S129F mutations. These R176Q and R179Q substitutions from ADHR patients are known to stabilize the full-length protein by interruption of a consensus 176RXXR179 furin-like proteolytic site (1, 22). Interestingly, introduction of the ADHR mutations conferred an increased resistance to proteolytic degradation of the secreted intact S71G and S129F mutant FGF23 proteins (Fig. 5). In the S129F mutant, the (R176 + 179Q) double mutation improved the secretion of the intact protein compared with the (R176Q) mutation alone indicating a “dose-dependent” rescue from degradation by furin-like enzymes (Fig. 5). However, introduction of the ADHR mutations did not fully correct the intracellular entrapment in any of the mutant proteins, as demonstrated by unchanged immunoreactivity in the cell lysates (Fig. 5). Taken together, these data indicate that furin-type enzymes are most likely responsible for the initial degradation of both S71G and S129F mutant FGF23, although resistance to proteolysis by these enzymes does not completely return secretion of FGF23 mutants to the levels of the wild-type protein.

#### Proteolysis of wild-type and mutant FGF23 protein

As introduction of the ADHR mutations rescued secretion of the intact S71G and S129F mutant proteins (Fig. 5), we speculated that the structural properties of TC-mutant FGF23 would also be stabilized by introduction of the ADHR mutations. In this regard, to produce polypeptides for analysis, we transiently expressed the native protein with a single ADHR mutation at position 176 [(S71S)(R176Q)] as well as the TC-mutant (S71G)(R176Q) and (S129F)(R176Q) FGF23 proteins, and compared their sensitivity to protein digestion by trypsin. Interestingly, neither the (S71G)(R176Q) nor the

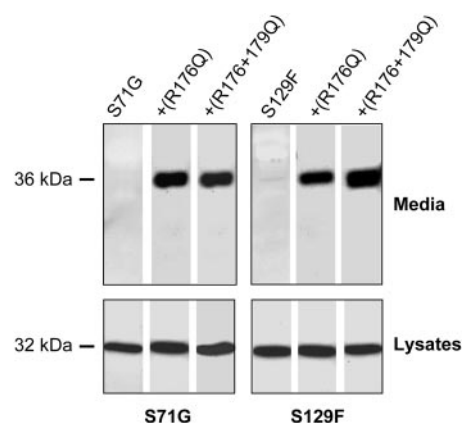


FIG. 5. Rescue of mutant FGF23 by disrupting the RXXR motif. The R176Q or (R176 + 179Q) mutations present in ADHR patients, known to disrupt the furin-like endopeptidase consensus RXXR motif, were coexpressed in tandem with either S71G or S129F mutant FGF23. Expression of either the single R176Q or the double (R176 + 179Q) mutations rescued the secretion of the intact S71G mutant. However, the secretion was not fully restored in either mutant, as indicated by the presence of the 32-kDa band in the cell lysates. Media were concentrated 10 times.

(S129F)(R176Q) mutant revealed increased sensitivity to trypsin digestion compared with the (S71S)(R176Q) protein, as determined by the disappearance of the intact 36-kDa band as a function of total protein concentration (Fig. 6). Both the (S71S)(R176Q), as well as the TC-mutant (S71G)(R176Q) and (S129F)(R176Q) FGF23s, were equally digested in the concentration range of 8–16 ng/ $\mu$ l of trypsin (Fig. 6). These data further suggest that the S71G and S129F mutants are stabilized by disrupting the RXXR motif recognized by furin-like endoproteases, thus allowing more efficient secretion of intact protein. Moreover, the presumable difference in folding of both mutants does not appear to generate additional trypsin cleavage sites compared with the wild-type protein, as we only detected a single protein species (Fig. 6).

#### Temperature rescue of intact S71G and S129F mutant FGF23

To examine the effect of the TC mutations on protein folding and assembly, we explored the possibility of rescuing S71G and S129F FGF23 with low temperature cell culture conditions. Cellular chaperone proteins are capable of distinguishing native and nonnative states of proteins, and thus target incorrectly folded proteins to degradative pathways (27). Occasionally, a misfolded polypeptide arising from mutations can be rescued from degradation under low-temperature conditions by chaperone proteins. These chaperones allow partial correction of improper folding of the mature protein, as in the case of cystic fibrosis transmembrane conductance regulator (28) and the V2 vasopressin receptor mutants (29). Therefore, transiently transfected cells expressing wild-type, S71G, or S129F FGF23 mutants were incubated in parallel at either 37 or 29 C, and conditioned media were

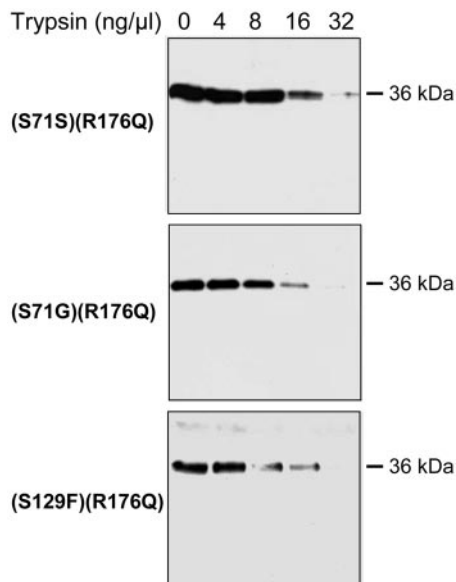


FIG. 6. Trypsin digestions of wild-type and mutant FGF23. (S71S)(R176Q) FGF23, (S71G)(R176Q) FGF23 and, (S129F)(R176Q) FGF23 proteins were subjected to trypsin digestion. Both the S71G and S129F FGF23 mutants displayed similar sensitivity to trypsin compared with S71S FGF23, as measured by the disappearance of the intact 36-kDa band. Media containing the mutants were concentrated 10 times.

analyzed by Western blotting. Interestingly, the S71G mutant was rescued at 29 C and secreted into the medium when compared with cells grown at 37 C (Fig. 7). However, protein structure was not fully corrected in this mutant as indicated by the presence of S71G FGF23 in the cell lysates during growth at 29 C (Fig. 7). In contrast, S129F mutant FGF23 revealed no immunoreactivity in the media at 29 or 37 C. However, the cell lysates were positive for the 32-kDa band, indicating that intact S129F protein was indeed expressed, although not secreted into the medium (Fig. 7). These data suggest that the S71G FGF23 is misfolded; however, the structural changes in the S71G mutant are capable of being corrected, and thus the mature S71G protein will escape intracellular entrapment by folding corrections made by low temperature. Moreover, the inability to rescue the S129F mutant protein may imply that this mutation is more destabilizing than the S71G, and that the changes in the protein structure of these two mutants are different. These observations are certainly consistent with our SIFT analysis and molecular modeling that indicate that the S129F mutant may be less stable than the S71G mutant, and also our finding that the S129F mutant produced lower levels of intact FGF23 *in vitro* compared with the S71G mutant protein (Fig. 4).

#### Discussion

FGF23 is a key regulator of Pi homeostasis and vitamin D metabolism, as demonstrated by the ADHR syndrome (1), and the fact that targeted deletion of the *Fgf23* gene (13, 14) or the administration of neutralizing FGF23 antibodies *in vivo* induces hyperphosphatemia (30). Herein, we present evidence that two different FGF23 mutations causing TC are destabilizing, and thus lead to decreased serum levels of intact FGF23 and development of the TC syndrome. Interestingly, heterozygous S/G family members displayed normal Pi and 1,25-(OH)<sub>2</sub>D<sub>3</sub> levels, indicating that one normal FGF23 gene copy is sufficient to maintain

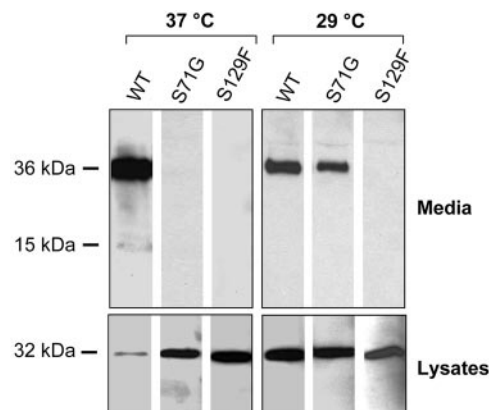


FIG. 7. Temperature rescue of mutant FGF23. Cells transfected with wild-type or mutant FGF23 were grown at either 37 or 29 C for 48 h. Wild-type FGF23 demonstrated lower expression when grown at 29 C. The S71G mutant displayed a partial rescue and secreted into the media during the lower temperature conditions; however, the S129F mutant was not secreted at either temperature (*upper panel*). Corresponding cell lysates are presented in the *lower panel*. Media were concentrated five times.



the regulation of Pi and vitamin D homeostasis as in the case of the *Fgf23* null mice (13, 14). In agreement, serum intact FGF23 levels were within the normal reference range in the heterozygous S/G carriers, as contrasted by the two homozygous G/G individuals, who displayed low intact, but remarkably high C-terminal levels of FGF23 (18). Therefore the apparently normal phenotype in S/G family members, apart from the mild increase in C-terminal FGF23 fragments, implies that the severity of the disease phenotype is negatively correlated to the amounts of circulating full-length FGF23 protein, providing further evidence for the physiologic relevance of FGF23 in maintaining a normal Pi balance.

The fact that inactivating mutations in the *GALNT3* gene, which encodes an enzyme involved in O-linked glycosylation, cause a similar phenotype to that of TC patients with *FGF23* mutations (31) raises the question whether the S71G and S129F *FGF23* mutations primarily give rise to a structural defect or to an altered glycosylation of FGF23. Because changes in structure and glycosylation are two interdependent processes, it is difficult to separate which of the two cellular events results in cleavage of FGF23 in TC patients harboring *FGF23* mutations. However, we present multiple lines of evidence indicating that structural changes are responsible, at least in part, for the apparent loss-of-function mechanism. First, both FGF23 mutants possess an inherent defect in secretion and are captured intracellularly (Fig. 3), a common feature of misfolded proteins (28). These data are in agreement with the findings of Benet-Pagés *et al.* (19) who recently demonstrated that S71G mutant FGF23 were retained within the Golgi complex. Second, molecular modeling predicts that S71G and S129F substitutions disrupt important interactions with several other residues, most likely affecting local protein folding. Finally, the S71G mutant is rescued when produced at 29°C, indicating that changes in folding of this mutant protein is at least partially restored during low-temperature conditions (Fig. 7). Because the serine residues 71 and 129 do not constitute predicted glycosylation motifs (18), we conclude that these TC mutations likely disrupt the native conformation leading to destabilization of the intact protein. However, we cannot rule out the possibility that conformational changes of S71G and S129F *FGF23* mutants prevent glycosylation at other residues than the S71 and S129, thereby contributing to structural changes. Indeed, introduction of any of the known mutations in ADHR patients are likely to influence O-linked glycosylation as the attachment sites are close to the RXXR motif (26).

Notably, individuals heterozygous for *GALNT3* mutations may present with subtle biochemical abnormalities, such as hyperphosphatemia and/or elevated 1,25-(OH)<sub>2</sub>D<sub>3</sub> levels (32), which were not found in the heterozygous individuals of our TC family (Table 1). The phenotypic discrepancies between heterozygous *FGF23* and *GALNT3* TC patients could be explained by the fact that mutations in *GALNT3* may lead to complete failure to glycosylate FGF23, whereas the *FGF23* mutations in TC may only lead to a partial glycosylation defect at specific residues due to improper folding of the FGF23 mutant

protein. Interestingly, to date it has been demonstrated that TC patients of Caucasian or Asian origin only harbor *FGF23* mutations (18–20), whereas African-American and Druze TC patients carry mutations in the *GALNT3* gene (31, 32). Therefore, it is also possible that the phenotypic discrepancy between heterozygous *FGF23* and *GALNT3* TC patients are due to differences in race- or background-specific genes. Indeed, differences in serum Pi levels between races have been reported (33).

In humans, serum FGF23 is elevated during chronic hyperphosphatemia associated with renal failure (6, 34), and it appears that serum FGF23 levels are altered during dietary changes in Pi intake, although much less pronounced than in mice (34–37). Our findings support the hypothesis that FGF23 production is stimulated by high serum Pi levels as homozygous G/G TC patients are severely hyperphosphatemic. This elevation in serum Pi would then stimulate FGF23 production, and is reflected by the markedly elevated C-terminal FGF23 levels. Conversely, S/G family members appear to have normal serum Pi and their C-terminal FGF23 concentrations are only discretely elevated compared with family members with two *FGF23* wild-type alleles. This difference could be due to compensatory increased transcriptional activity of *FGF23*. Alternatively, the markedly elevated serum C-terminal FGF23 levels in G/G TC patients may be due to an increased proteolytic degradation of S71G mutant FGF23 into C-terminal fragments. Although this mechanism probably contributes to the low ratio of intact *vs.* C-terminal FGF23 in TC, it is still not likely to account for the magnitude of C-terminal fragments observed in G/G TC patients, as then an intermediate elevation of these fragments would be expected in all S/G heterozygote individuals of our TC family. Importantly, the elevation of C-terminal fragments in carriers may indicate minor up-regulation of FGF23 in response to slightly higher serum Pi concentrations, which may be relevant to these individuals in situations of Pi challenge or decreased renal Pi excretion, such as during hypoparathyroidism or renal failure.

Importantly, the secretion of intact S71G and S129F mutants was rescued by the introduction of the R176Q or (R176Q + 179Q) mutations found in ADHR that are known to disrupt the RXXR motif recognized by furin-like endopeptidases (Fig. 5). The extent to which the FLAG tag influences FGF23 folding and processing is difficult to determine; however, the fact that the S71G and S129F mutants are processed similarly, and rescued similarly by the ADHR mutations, most likely rules out major effects of the FLAG residues. These results revealed a critical role for furin-like enzymes in the proteolytic cleavage of mutant FGF23 in TC patients; however, they may also be important for understanding the pathogenesis of ADHR. Of significance, the primary molecular defect in ADHR is most likely structural, as the missense mutations at residues R176 and R179 prevent proteolytic cleavage by furin-like enzymes, which then may increase circulating intact FGF23 concentrations (22). Although the primary defect in FGF23 is structural, the ADHR missense mutations in FGF23 may, however, cause a misglycosylation of FGF23, as demonstrated previously by mass spectrometry (26). Consequently, when the FGF23-producing cell senses the

defective glycosylation, or differential folding of FGF23 due to misglycosylation, the cell is unable to remove the ADHR mutant FGF23 by proteolytic processing because the R176 and R179 mutations inhibit furin-like cleavage. This model is consistent with the fact that the S71G and S129F mutants, which are predicted to have altered structural characteristics (Figs. 5 and 6), can be partially rescued by interruption of the RXXR motif in FGF23. Therefore, it is possible that furin-like enzymes may act as intracellular “quality control monitors”, allowing correctly folded and posttranslationally modified FGF23 to be normally secreted, whereas the furins more efficiently recognize and cleave improperly folded or processed FGF23 as in the case of TC.

In summary, the genotype-phenotype correlations of our TC family demonstrate that only homozygote G/G individuals display a disease phenotype but that heterozygote carriers of the S/G mutation do have modestly increased C-terminal FGF23 fragments. The S71G and S129F mutant FGF23 proteins causing TC are differentially processed, most likely due to altered protein conformations, and the destabilizing nature of these mutations likely leads to low circulating levels of biologically active intact FGF23. Thus, FGF23 has a profound impact on normal physiology of Pi and vitamin D metabolism as exemplified by the TC syndrome.

### Acknowledgments

We thank Jeffrey Lavigne and Richard Zahradnik (Immutopics, Inc.) for supplying the C-terminal FGF23 antibodies.

Received April 13, 2005. Accepted June 5, 2005.

Address all correspondence and requests for reprints to: Kenneth E. White, Ph.D., 975 West Walnut Street, IB130, Indiana University School of Medicine, Indianapolis, Indiana 46202. E-mail: kenewhit@iupui.edu.

This work was supported by National Institutes of Health Grant DK063934 (to K.E.W.), the Henning and Johan Throne-Holst Foundation, the Swedish Society of Medicine, as well as the Indiana Genomics Initiative; supported in part by Lilly Endowment, Inc. H.J.G. is supported by National Institutes of Health Grant T32 AR007581.

### References

- ADHR Consortium 2000 Autosomal dominant hypophosphatemic rickets is associated with mutations in FGF23. *Nat Genet* 26:345–348.
- Bianchini JW, Stambler AA, Harrison HE 1971 Familial hypophosphatemic rickets showing autosomal dominant inheritance. *Birth Defects Orig Artic Ser* 7:287–295.
- Econs MJ, McEnery PT 1997 Autosomal dominant hypophosphatemic rickets/osteomalacia: clinical characterization of a novel renal phosphate-wasting disorder. *J Clin Endocrinol Metab* 82:674–681.
- Yamazaki Y, Okazaki R, Shibata M, Hasegawa Y, Satoh K, Tajima T, Takeuchi Y, Fujita T, Nakahara K, Yamashita T, Fukumoto S 2002 Increased circulatory level of biologically active full-length FGF-23 in patients with hypophosphatemic rickets/osteomalacia. *J Clin Endocrinol Metab* 87:4957–4960.
- Jonsson KB, Zahradnik R, Larsson T, White KE, Sugimoto T, Imanishi Y, Yamamoto T, Hampson G, Koshiyama H, Ljunggren O, Oba K, Yang IM, Miyauchi A, Econs MJ, Lavigne J, Juppner H 2003 Fibroblast growth factor 23 in oncogenic osteomalacia and X-linked hypophosphatemia. *N Engl J Med* 348:1656–1663.
- Weber TJ, Liu S, Indridason OS, Quarles LD 2003 Serum FGF23 levels in normal and disordered phosphorus homeostasis. *J Bone Miner Res* 18:1227–1234.
- Bai XY, Miao D, Goltzman D, Karaplis AC 2003 The autosomal dominant hypophosphatemic rickets R176Q mutation in fibroblast growth factor 23 resists proteolytic cleavage and enhances in vivo biological potency. *J Biol Chem* 278:9843–9849.
- Shimada T, Mizutani S, Muto T, Yoneya T, Hino R, Takeda S, Takeuchi Y, Fujita T, Fukumoto S, Yamashita T 2001 Cloning and characterization of FGF23 as a causative factor of tumor-induced osteomalacia. *Proc Natl Acad Sci USA* 98:6500–6505.
- Shimada T, Hasegawa H, Yamazaki Y, Muto T, Hino R, Takeuchi Y, Fujita T, Nakahara K, Fukumoto S, Yamashita T 2004 FGF-23 is a potent regulator of vitamin D metabolism and phosphate homeostasis. *J Bone Miner Res* 19:429–435.
- Larsson T, Marsell R, Schipani E, Ohlsson C, Ljunggren O, Tenenhouse HS, Juppner H, Jonsson KB 2004 Transgenic mice expressing fibroblast growth factor 23 under the control of the  $\alpha 1(I)$  collagen promoter exhibit growth retardation, osteomalacia, and disturbed phosphate homeostasis. *Endocrinology* 145:3087–3094.
- Shimada T, Urakawa I, Yamazaki Y, Hasegawa H, Hino R, Yoneya T, Takeuchi Y, Fujita T, Fukumoto S, Yamashita T 2004 FGF-23 transgenic mice demonstrate hypophosphatemic rickets with reduced expression of sodium phosphate cotransporter type IIa. *Biochem Biophys Res Commun* 314:409–414.
- Bai X, Miao D, Li J, Goltzman D, Karaplis AC 2004 Transgenic mice overexpressing human fibroblast growth factor 23 (R176Q) delineate a putative role for parathyroid hormone in renal phosphate wasting disorders. *Endocrinology* 145:5269–5279.
- Sitara D, Razzaque MS, Hesse M, Yoganathan S, Taguchi T, Erben RG, Juppner H, Lanske B 2004 Homozygous ablation of fibroblast growth factor-23 results in hyperphosphatemia and impaired skeletogenesis, and reverses hypophosphatemia in Phex-deficient mice. *Matrix Biol* 23:421–432.
- Shimada T, Kakitani M, Yamazaki Y, Hasegawa H, Takeuchi Y, Fujita T, Fukumoto S, Tomizuka K, Yamashita T 2004 Targeted ablation of Fgf23 demonstrates an essential physiological role of FGF23 in phosphate and vitamin D metabolism. *J Clin Invest* 113:561–568.
- Inclan A, Leon P, Carnejo MG 1943 Tumoral calcinosis. *J Am Med Assoc* 121:490–495.
- Prince MJ, Schaeffer PC, Goldsmith RS, Chausmer AB 1982 Hyperphosphatemic tumoral calcinosis: association with elevation of serum 1,25-dihydroxycholecalciferol concentrations. *Ann Intern Med* 96:586–591.
- Mitnick PD, Goldfarb S, Slatopolsky E, Lemann Jr J, Gray RW, Agus ZS 1980 Calcium and phosphate metabolism in tumoral calcinosis. *Ann Intern Med* 92:482–487.
- Larsson T, Yu X, Davis SI, Draman MS, Mooney SD, Cullen MJ, White KE 2005 A novel recessive mutation in fibroblast growth factor-23 causes familial tumoral calcinosis. *J Clin Endocrinol Metab* 90:2424–2427.
- Benet-Pagés A, Orlik P, Strom TM, Lorenz-Depiereux B 2005 An FGF23 missense mutation causes familial tumoral calcinosis with hyperphosphatemia. *Hum Mol Genet* 14:385–390.
- Araya K, Fukumoto S, Backenroth R, Takeuchi Y, Nakayama K, Ito N, Yamazaki Y, Yamashita T, Silver J, Igarashi T 2004 A mutation in FGF-23 gene enhances the processing of FGF-23 protein and causes tumoral calcinosis. *J Bone Miner Res* 19:541.
- Li Voon Chong SW, Ah Kion S, Cullen MJ 1999 A report of familial hyperphosphatemia in an Irish family. *Ir J Med Sci* 168:262–264.
- White KE, Jonsson KB, Carn G, Hampson G, Spector TD, Mannstadt M, Lorenz-Depiereux B, Miyauchi A, Yang IM, Ljunggren O, Meitinger T, Strom TM, Juppner H, Econs MJ 2001 The autosomal dominant hypophosphatemic rickets (ADHR) gene is a secreted polypeptide overexpressed by tumors that cause phosphate wasting. *J Clin Endocrinol Metab* 86:497–500.
- Harmer NJ, Pellegrini L, Chirgadze D, Fernandez-Recio J, Blundell TL 2004 The crystal structure of fibroblast growth factor (FGF) 19 reveals novel features of the FGF family and offers a structural basis for its unusual receptor affinity. *Biochemistry* 43:629–640.
- Pieper U, Eswar N, Braberg H, Madhusudhan MS, Davis FP, Stuart AC, Mirkovic N, Rossi A, Marti-Renom MA, Fiser A, Webb B, Greenblatt D, Huang CC, Ferrin TE, Sali A 2004 MODBASE, a database of annotated comparative protein structure models, and associated resources. *Nucleic Acids Res* 32:D217–D222.
- White KE, Carn G, Lorenz-Depiereux B, Benet-Pagés A, Strom TM, Econs MJ 2001 Autosomal-dominant hypophosphatemic rickets (ADHR) mutations stabilize FGF-23. *Kidney Int* 60:2079–2086.
- Shimada T, Muto T, Urakawa I, Yoneya T, Yamazaki Y, Okawa K, Takeuchi Y, Fujita T, Fukumoto S, Yamashita T 2002 Mutant FGF-23 responsible for autosomal dominant hypophosphatemic rickets is resistant to proteolytic cleavage and causes hypophosphatemia in vivo. *Endocrinology* 143:3179–3182.
- Welch WJ 2004 Role of quality control pathways in human diseases involving protein misfolding. *Semin Cell Dev Biol* 15:31–38.
- Denning GM, Anderson MP, Amara JF, Marshall J, Smith AE, Welsh MJ 1992 Processing of mutant cystic fibrosis transmembrane conductance regulator is temperature-sensitive. *Nature* 358:761–764.
- Morello JP, Salahpour A, Laperriere A, Bernier V, Arthus MF, Lonergan M, Petaja-Repo U, Angers S, Morin D, Bichet DG, Bouvier M 2000 Pharmacological chaperones rescue cell-surface expression and function of misfolded V2 vasopressin receptor mutants. *J Clin Invest* 105:887–895.
- Shimada T, Yamazaki Y, Aono Y, Hasegawa H, Hino R, Takeuchi Y, Fujita T, Fukumoto S, Yamashita T 2003 Neutralization of intrinsic FGF-23 action by antibodies reveal the essential role of FGF-23 in physiological phosphate and vitamin D metabolism. *J Bone Miner Res* 18:597.
- Topaz O, Shurman DL, Bergman R, Indelman M, Ratajczak P, Mizrahi M,



- Khamaysi Z, Behar D, Petronius D, Friedman V, Zelikovic I, Raimer S, Metzker A, Richard G, Sprecher E 2004 Mutations in GALNT3, encoding a protein involved in O-linked glycosylation, cause familial tumoral calcinosis. *Nat Genet* 36:579–581
32. Ichikawa S, Lyles KW, Econs MJ 2005 A novel GALNT3 mutation in a pseudoautosomal dominant form of tumoral calcinosis: evidence that the disorder is autosomal recessive. *J Clin Endocrinol Metab* 90:2420–2423
33. Specker BL, Lichtenstein P, Mimouni F, Gormley C, Tsang RC 1986 Calcium-regulating hormones and minerals from birth to 18 months of age: a cross-sectional study. II. Effects of sex, race, age, season, and diet on serum minerals, parathyroid hormone, and calcitonin. *Pediatrics* 77:891–896
34. Larsson T, Nisbeth U, Ljunggren O, Juppner H, Jonsson KB 2003 Circulating concentration of FGF-23 increases as renal function declines in patients with chronic kidney disease, but does not change in response to variation in phosphate intake in healthy volunteers. *Kidney Int* 64:2272–2279
35. Allen H, Whybro A, Barker M 2002 Endocrine response to escalating-dose phosphate supplementation in men: is FGF-23 phosphatonin? *J Bone Miner Res* 17:S159
36. Burnett SM, Gunawardene S, Bringham FR, Juppner H, Finkelstein JS 2004 The effects of dietary phosphate on the regulation of FGF-23 in humans. *J Bone Miner Res* 19:S252
37. Ferrari SL, Bonjour JP, Rizzoli R 2005 Fibroblast growth factor-23 relationship to dietary phosphate and renal phosphate handling in healthy young men. *J Clin Endocrinol Metab* 90:1519–1524

*Endocrinology* is published monthly by The Endocrine Society (<http://www.endo-society.org>), the foremost professional society serving the endocrine community.